

4.1 Introduction

4.1.1 Elimination of noises in ECG signal for European ST-T and MIT-BIH database using SG filter

Electrodes are attached to the skin to capture ECG signals at specific locations on the human body, as discussed in Chapter 1. Artifacts (anything other than muscle action of the heart) are introduced into the ECG during recording. Baseline wandering (B.W.) and muscular tremors are the most typical artifacts. These artifacts hurt the Electrocardiogram and make accurate delineation of characteristic waves more challenging because the baseline wander pattern occurs in the S.T. segment of the Electrocardiogram, muscle tremors mimic the iso-electric line, and misrepresent all segments of the Electrocardiogram. Eliminating ECG artifacts aims to use developed techniques to make identifying the Electrocardiogram's distinctive waves simpler and more accurate.

Many medical applications depend on accurate delineation, including identifying the QRS complex, classifying ectopic rhythms, studying clinical irregular heartbeat, treating myocardial ischemia, heart rate variability, and electrographic signal data reduction: filters [U.M. Chaskar et al., 2009], wavelet-based de-noising [G. Kaushik et al., 2012; T. Gandhi et al., 2011], neural network-based [M.E. Cohen et al., 2006], and nonlinear signal processing [U.R. Acharya et al., 2013] have all been described in the literature in the last few years for the removal of artifacts. Based on the analysis, linear prediction based [J. Makhoul, 1975], principal component analysis (PCA) based [R. Duda et al., 2001], linear discriminant analysis (LDA) based [R. Duda et al., 2001], independent component analysis (ICA) [A. Hyvärinen, J. Karhunen and E. Oja et.al, 2001], Fourier transform [D.L. Fugel, 2009], power spectral density. Filters [U.M. Chaskar et al., 2009], wavelet-based de-noising [G. Kaushik, 2012; T. Gandhi et al., 2011], neural network-based [M.E. Cohen, 2006], and nonlinear signal processing [U.R. Acharya, 2013] have all been described in the literature in the last few years for the removal of artifacts. For example, digital infinite impulse response (IIR) filters have been employed to remove noise from ECG recordings. Signals [S.C. Mahesh, 2008]. IIR filters are simple to design, and even higher-order IIR filters

function well. Still, they demand more memory due to the long filtering time and are not ideal for filtering highly nonlinear physiological ECG signals. Power line interference can also be eliminated using the dynamic median filter [S.M.M. Martens et al., 2006; F.C. Chang et al., 2007]. Due to its reduced residual errors and quicker reaction time, this method is preferable for eliminating noise [S.G. Tareen, 2008].

The received signal information is necessary to achieve successful filtering using this method. For de-noising E.C.G. signals for P.L.I., typical and efficient ways include notch filters [M.S. Chavan et al., 2008] and finite impulse response (F.I.R.) filters [J.A. Van Alste and T.S. Schilder, 1985; C.B. Mbachu et al., 2011] are used. Unfortunately, the outcomes of these filtering techniques have been disappointing. Another technique for removing artifacts is the averaging filter [M.R. Rangaraj, 2002], although it requires a large number of time frames. For the elimination of these sounds in E.C.G. signals, researchers have used independent component analysis (I.C.A.) [M.P.S. Chawla et al., 2008; T. He, G. Clifford, and L. Tarassenko, 2006; A.K. Barros et al., 1998].

I.C.A., on the other hand, does not support competent filtering based on prior information from processed signals. P.L.I. has also been used with advanced techniques like empirical mode decomposition [M.C.Z. Zhidong, 2008], neural networks [J. Mateo et al., 2008], P.C.A. [M.P.S. Chawla, 2011], and wavelet transform [M. Kania et al., 2007]. Wavelets [I.A. Dotsinsky and G.S. Mihov, 2008; P. Augustyniak, 2006; D.D. Raghavendra, 2012; A. Graps, 1995] and singular value decomposition (S.V.D.) filters [J. S. Paul et al., 2000] have been studied for the elimination of muscular tremors in E.C.G. Similarly, linear filtering [I. Markovsky et al., 2012] is used to fix baseline wanders in the frequency range of 0.5 Hz to 1 Hz.

The Gibbs phenomenon is produced as a result of this procedure. Polynomial approximation, or cubic spline filtering, was created to overcome this problem. [J.R. Laguna et.al, 1992]. Time-varying digital filters [L. Sornmo, 1993], digital filters [N. Henzel, 2006], the Projection Pursuit Gradient Ascent Algorithm [U. Zahoor and A.O. Farooq, 2009], wavelet transforms [K. Daqrouq, 2005; N.H. Poojya Doddappa, S. Mukherjee, 2011; E.B. Lin et al., 2013; O. Sayadi and M.B. Shamsollahi, 2007]. The wavelet and genetic algorithms [E.S.A.El. Dahshan, 2011] were used in the implementation. This report [F.A. Afsar, 2009] can be used to compare baseline

wander removal techniques. Although P.C.A., I.C.A., and N.N. approaches are used to extract artifacts from E.C.G. signals using band selection, Unless the basis-functions are received training on electrocardiogram (E.C.G.) data, these techniques are sensitive to minor modifications in either the input signal or the artifact. Understanding the artifacts and their frequency in the recorded E.C.G. signal is critical. As a result, the time-frequency analysis-based wavelet transform is chosen to address the limitations of various methods for removing artifacts from ECG.

In MATLAB, numerous wavelet functions can be used to de-noise ECG signals. The detail coefficients (cD) and approximate coefficients (cA) are generated independently by the wavelet transform [A.K. Manocha and M. Singh, 2013]. Choosing the proper wavelet function and thresholding procedure is critical when de-noising ECG signals. Several researchers have used various performance analysis approaches to evaluate their developed products, as shown in Figure 4.1.

Kurtosis [L.N. Sharma et al., 2013], percentage root mean square difference (PRD), positive predictivity standard deviation, sensitivity, signal-to-noise ratio (SNR), root mean square error (RMSE), and distortion measurement are some algorithms.

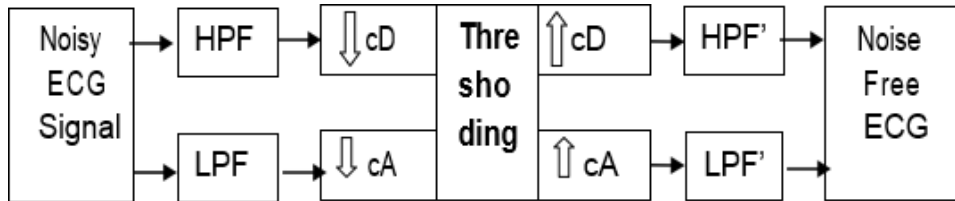


Figure 4.1 The wavelet decomposition and reconstruction procedure [Reproduced from L.N. Sharma et.al, 2013]

4.1.2 Wavelet Thresholding

Wavelet Thresholding is a technique for determining the size of a wave. It is an estimating method that takes advantage of the ability to de-noise any form of artifact in acquiring a non-stationary ECG signal. As illustrated in Figure 4.2, there are two types of thresholding: hard and soft thresholding. Hard thresholding, according to Eqn. 4.1, is much more susceptible to changes in the amplitude and thus more uncertain. Soft thresholding has a higher bias because significant wavelet coefficients shrink after decomposition. Eqn. 4.2 proves that soft thresholding is more stable than hard thresholding. Hard thresholding sets all coefficients to zero for X_{dh} less than T , but soft thresholding does the opposite for X_{ds} less than T and subtracts T from the

signal above T . Several studies have shown that de-noising ECG signals with soft thresholding yields better results.

$$X_{dh} = \begin{cases} 0 & x < T \\ x & x \geq T \end{cases} \quad (4.1)$$

$$X_{ds} = \begin{cases} x - T & x > T \\ 0 & x \leq T \end{cases} \quad (4.2)$$

$$x + T \quad x < -T$$

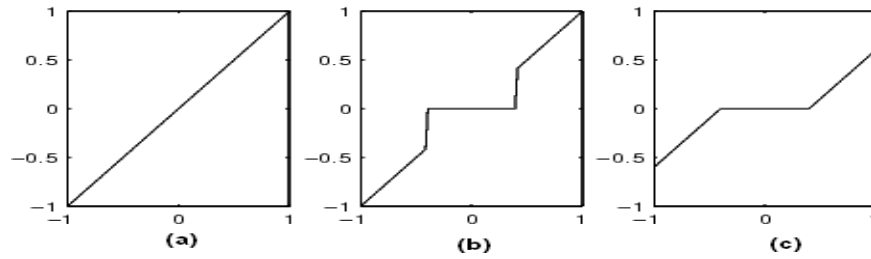


Figure 4.2 a) Input signal b) Hard threshold signal c) Soft threshold signal

[reproduced from <http://in.mathworks.com/help/wavelet/ref/wthresh.html>]

4.1.3 Technique for De-noising of Electrocardiogram Signals

Figure 4.3 shows a flow chart of an algorithm to remove noises in the ECG. We have proposed the wavelet transform (db_4) is employed to decompose the electrocardiogram (ECG) message into detailed coefficients ($Cd_1, Cd_2, \dots, Cd_{10}$) and approximate coefficients ($Ca_1, Ca_2, \dots, Ca_{10}$) up to the tenth level. Ca_9 and Ca_{10} have low-frequency signals with ranges similar to baseline wander, while Cd_1 and Cd_2 have high-frequency information. So, by employing wavelet transform, the coefficients (Ca_9, Ca_{10} , and Cd_1, Cd_2) are rejected. Keep the remaining coefficients as they are because they constitute essential information. Wavelet features are frequently used to retrieve an input signal from a noisy signal; the first stage, analysis, is choosing a suitable wavelet. The second step uses the wavelet function to decompose a noisy signal. The decomposition signal's vectors are obtained as detail and approximate coefficients following decomposition. The approximate coefficients are the decomposed signal with high-scale and low-frequency vectors, whereas the detail coefficients are the high-frequency, low-scale vectors. For the next iteration, the approximated coefficients are used as input. This cycle is repeated until the required level is reached. The third step, the thresholding step, attempts to measure detail or approximation coefficients established by the wavelet. The type of artifacts determines whether hard or soft thresholding is used, and the final step is to use the inverse wavelet transform to reconstruct a signal with the same level of

decomposition.

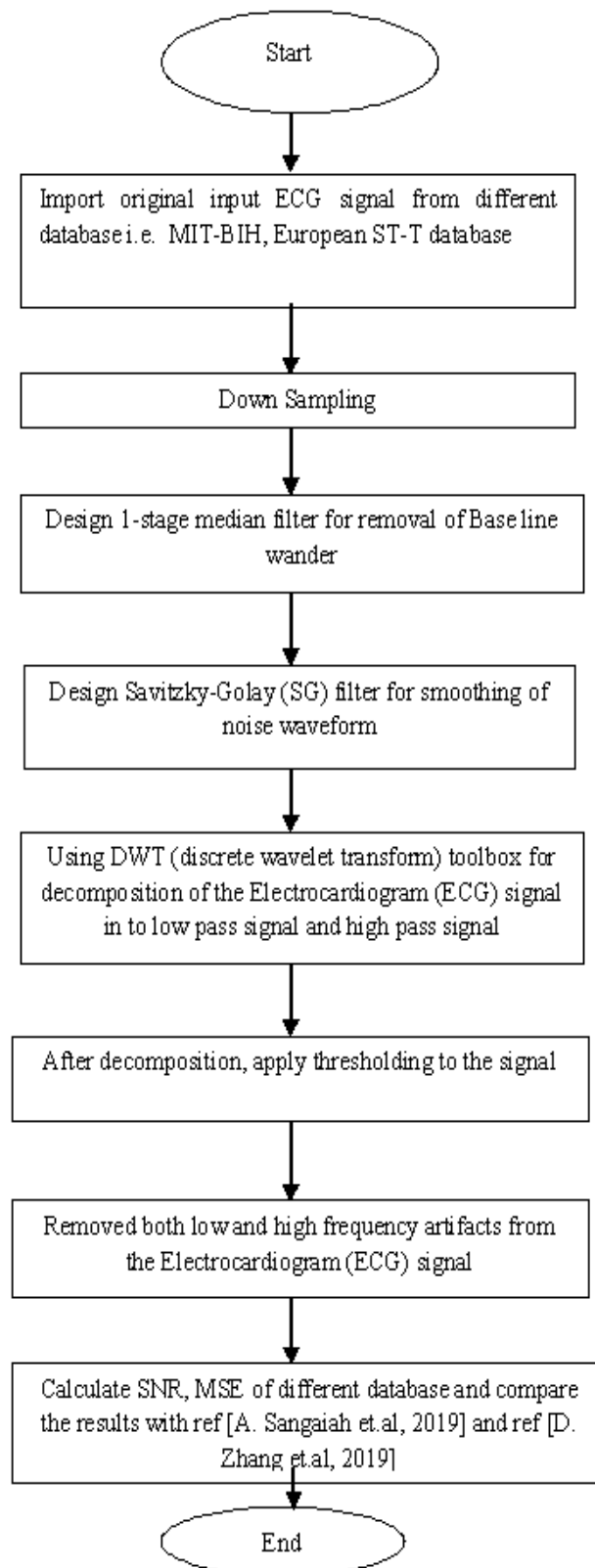


Figure 4.3 shows a flow chart of an algorithm for removal of noises in the ECG signal

4.2 Detection of Characteristics Point of Electrocardiogram (ECG) Signal

The automatic process of identifying ECG properties, such as amplitudes and time intervals, is called ECG delineation. The proper definition of delineation indicates the precise location of a signal's border. In the instance of ECG, this entails first recognizing the R peaks in the movement. Then, surrounding the identified R peak, windows are defined for recognizing the QRS complex and other distinctive points such as the P wave, T wave, and S.T. segment. Many algorithms have been reported for feature extraction of distinctive spots in the ECG. Many algorithms for detecting ECG's QRS have been published in the literature. For example, wavelet-based QRS detection [C. Saritha et al., 2008], the Pan and Tomkins method in assembly language [J. Pan and W.J. Tomkins, 1985], software-based QRS detection [O. Pahlm and L. Sornmo, 1984], and mathematical models-based QRS detection [F. Gritzali, 1988; A. Ghaffari et.al, 2008]. It is possible to review the concepts of software QRS detection [B.U. Kohler et al., 2002]. Similarly, nine QRS detection methods [G.M. Friesen et al., 1990] may be compared. Other methods include matching filters [A.S.M. Koeleman et al., 1985], second-order derivatives

[J.G.C. Kemmelings et al., 1994], ECG slope criteria [I.K. Daskalov et.al, 1998], Hidden Markov Models (HMM) [M.J. Vaessen, 2006], Bayesian approach [C. Lin et al., 2010], wavelet transformations [A.K. Manocha, 2016] correlation-based delineation of ECG waves [A. Karimipour, M.R. Homaeinezhad et al., 2014], K-nearest neighbor-based algorithm for P and T waves delineation [I. Saini et al., 2014], a method based on the evolutionary optimization process [J. Dumont et al., 2010] support vector machine-based [S.S. Mehta and N.S. Lingayat, 2009], quality-supported analysis of characteristic templates [A. Karimipour and M.R. Homaeinezhad, 2014] methods have been carried out. For many reasons, researchers still struggle to develop an automated diagnosis system that accurately delineates the ECG. Like, the P wave is characterized by low amplitude and Muscle noise or electrode movements can go missed. The multi-resolution feature of wavelets transforms, which decomposes the signals in the required scales for accurate analysis of non-stationary signals [I. Daubechies, 1990; A. Graps, 1995; D.L. Fugel, 2009] is a boon for non-stationary ECG signals, according to a literature review [I. Daubechies, 1990; A. Graps, 1995, D.L. Fugel, 2009]. It is also necessary for correct delineation and analysis of ECG signals that the transform has an adequate resolution in both the

frequency and temporal domains. Many frequency-time analysis approaches for representing ECG signals are available in the literature, each with benefits and drawbacks. [R.J. Martis et al., 2011] discuss the advantages and disadvantages of various strategies. Employing a multi-resolution wavelet transform, which integrates the feature of varying time-frequency resolution over the time-frequency plane, is the best technique to evaluate non-stationary ECG signals. The rebuilt signal has about the same size and dimensions as the deconstructed signal, making wavelet transform a particularly potent signal processing approach. We devised and verified a new method for delineating ECG characteristic spots using the wavelet transform and the window search method.

4.2.1 Techniques for Detecting QRS for MIT-BIH Database

The ECG signals were converted to MATLAB format using the 360 Hz sampling frequency of the MIT-BIH arrhythmia database (.mat). It has 48 records of ECG signals with a length of 30 minutes and a resolution of 11 bits over a 10-mV range. Figure 4.4 displays the block diagram of the suggested QRS complex detection algorithm for ECG signal. It contains de-noising, QRS detection, R-peak detection, on and off peaks, and extraction of morphological parameters. MATLAB 2018 was used to implement the technique, and it was evaluated using the first channel's ECG readings (MLII). Our data processing took an average of 1.33 seconds for every 30 minutes of ECG data.

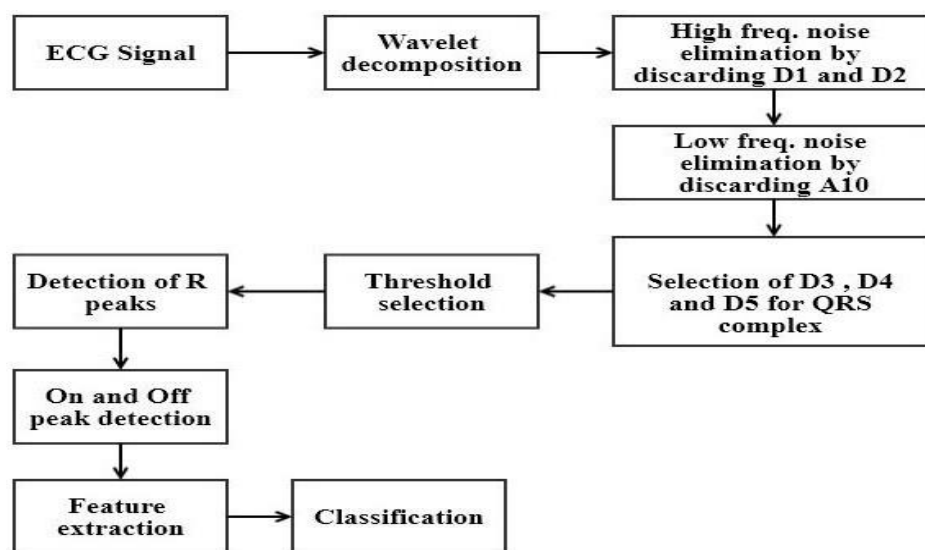


Figure 4.4 Block diagram of DWT-based ECG beat detection algorithm
[reproduced by C. Saritha, 2008]

4.3 Detection of Features of ECG Signal

T wave detection

A 200ms search window is set after the offset of the QRS complex to detect the T wave. Within this period, 22 maxima of $|x[n] W|$ are identified, and those exceeding the threshold T are considered T wave peaks. The onset and offset (zero crossing) points are located using the same lookup approach before and after the T wave peak. A scale of 24 is used to address problems in identifying the beginning and end of P and T waves caused by baseline drift and motion artifacts.

Maximums of $|x[n]W|$ 22 with amplitudes higher than T wave is considered significant wave gradients or T wave peaks. The following six potentials. T wave morphologies are discovered depending on the number and direction of the found maximum: positive (+), negative (-), bi-phasic (+/- or -/+), only upwards, and only downwards. If the T wave is not detected in scale 24, go back to $|x[n]W|$ 22 and repeat the process. T wave boundaries were determined using the same criteria as QRS onset and offset with thresholds on a scale of 2k.

P wave detection

The P wave is identified by placing the search window (200ms) well before QRS complex offset. Finding maxima $|x[n]W|$ 22 in that window; maxima values that exceed this threshold value T are deemed P wave peaks. The beginning and offset locations of the P wave, like the T wave, are also identified. P wave delineation: P wave drawing is performed in the same manner as T wave delineation.

Morphological features and statistical features are the two types of features that can be found.

4.3.1 Morphological Characteristics

The ECG's morphology is as follows: On the ECG, each heartbeat may be seen as a series of deflections away from the baseline. These deflections demonstrate the progression of electrical impulses in the heart, which creates muscular contraction. The letters P, Q, R, S, and T are widely used to define a single sinus (normal) Electrocardiogram cycle corresponding to one heartbeat. Morphological characteristics include:

- The QRS interval.

- T wave interval.
- P wave interval.
- R amplitude.
- R and S amplitude.
- QRS delineation interval.
- T wave delineation interval.
- P wave delineation interval.
- RR interval.

(a) Morphological features are

- QRS interval • T wave interval • P wave interval • R amplitude • R and S amplitude • P and Twave amplitude
- QRS delineation interval • T wave delineation interval • P wave delineation interval • RR interval
- ST slope

4.3.2 Statistical Characteristics

This phrase refers to various strategies for exploring, understanding, proving, and forecasting based on the most straightforward datasets acquired from populations using a sampling strategy. Statistical characteristics are defined as:

(b) Statistical Features are

- Mean
- Variance
- Standard deviation
- Skewness
- Kurtosis

Mean (μ)-The arithmetic average of the value in a data set is obtained by summing the values and dividing by the number of values in the set. The value of the mean is given in Eqn. (4.3)

$$\text{Mean} = \sum \frac{x_i}{n} \quad (4.3)$$

Variance (V)-The variance of data is the mathematical sum of squared deviations between the values and the mean. The value of variance is calculated by Eqn. (4.4)

$$\text{Variance (V) } (\sigma^2) = (\text{Standard Deviation})^2 \quad (4.4)$$

Standard Deviation (S.D.)- The standard deviation (SD) represents the amount of diversity or "dispersion" from the mean (mean, or expected value). A variance indicates that the data points are close to the average, whereas a high enough standard deviation indicates that the value points are distributed across a wide range of scales. It is equal to the square root of the variance given in Eqn. (4.5)

$$S.D = \sqrt{\sum \frac{(x_i - \text{mean})^2}{n}} \quad (4.5)$$

Here, $x_i = i^{\text{th}}$ beat denotes the total number of beats, and SD is the standard deviation is used for the measurement of absolute dispersion in the signal. It provides the facility for the calculation of a complete dataset.

Skewness (S)- is a concept that refers to asymmetry in distribution. Positively skewed to the right describes a distribution with an asymmetric tail reaching the right. Asymmetric tails extending to the left are also said to be negatively skewed to the left. Its objective is to verify and calculate data symmetry, as well as to indicate the probability of variable distribution.

The skewness value is calculated using Eqn. 4.6.

$$\text{Skewness} = E[x - \mu / \sigma]^3 \quad (4.6)$$

Kurtosis (C): This method measures the degree of flatness of a distribution by comparing it to a regular pattern to see if it is more attenuated or flattened. The higher the kurtosis, the more values out of the standard are present. The following definition of kurtosis is given in Eqn. (4.7).

$$\text{Kurtosis} = E[x - \mu / \sigma]^4 \quad (4.7)$$

4.4 The Proposed Classification of Arrhythmias Using Deep Learning

An electrocardiogram (ECG) is a healthcare monitoring test to measure the heart's electrical activity to assist doctors in detecting abnormal heart rhythms. Early categorization of ECG data is critical for determining therapy options for patients. An electrocardiogram is, in theory, a time series signal produced by the heart's electrical activity. Various methods have been used to classify these time series signals using machine learning algorithms. These methods necessitate feature extraction, leading to inconsistencies in the extracted features and variations in the ECG data. Deep learning techniques, such as methods based on Convolution Neural Networks (CNN), may be used to avoid manually creating characteristics from ECG signals.

The presence of an abnormal Electrocardiogram is an essential predictor of heart disease in both the elderly and the youth [D.D. He and C.G. Sodini, 2015]. Cardiovascular arrhythmia is a common illness that, if left untreated, can lead to abrupt death in some situations. Early detection of changes in heart activity using real-time monitoring aids in lifesaving and health care. Remembering that an abnormality in an individual's ECG is a temporary symptom is also essential. Because cardiac arrhythmia beats emerge quickly, hospitals cannot accurately diagnose arrhythmia. Furthermore, the traditional ECG monitoring system frequently employs a signal cable for connecting humans to the device and for tracking purposes. A direct wired connection is available, and a wearable gadget with remote monitoring of heart activity without interfering with the user's regular activities. The wearable device collects a large amount of data regularly. Cardiologists use the ECG waveform to diagnose anomalies depending on the number of cardiac rhythms and any changes in morphological patterns. However, because there are so many heartbeats, checking each one is impossible, which increases the complexity of the inspection and lowers the clinician's categorization accuracy [Y. Xia, H. Zhang et al., 2018]. Heartbeat Categorization with Electrocardiogram is a valuable method for researching heart arrhythmia, a bio-signal analysis issue [T. Teijeiro et al, 2018].

Arrhythmia is defined as a series of heartbeats with abnormal morphology or intervals. As a result, once the signal has been acquired, heartbeat categorization is the next important step. A human professional performs the long-term assessment, which is time-consuming and prone to fatigue-related mistakes. As a direct consequence, an automatic system for classifying heart rhythm is required, and identifying a person with irregular heartbeats necessitates the assistance of medical professionals. [P.D. Chazal and M.O. Dwyer, 2004]. The study focuses on arrhythmia categorization utilizing an individual's ECG signal to begin a precise diagnosis of the patient. Configured ideally with an optimization method, deep neural networks are used to conduct the arrhythmia classification. It's worth noting that the arrhythmia classification reduces time in doing successful classification, allowing for early arrhythmia identification. Feature extraction and feature classification are the next steps in the arrhythmia classification process. Initially, the ECG signal is processed to a multi-resolution wavelet-based technique to identify the wave components in ECG signals.

4.4.1 Convolution Neural Networks

This research uses training and learning neural networks to identify diverse data types. For classification purposes, CNN-based classification models were used in the current study. In general, CNNs are made up of convolution and pooling stages that aid in extracting relevant features from image maps [I. Mebsout, 2020]. A CNN model takes the input of a three-dimensional tensor, an image of RGB (Red, Green and Blue) value with width and height information. The neural network then goes to the additional processing steps with this input image. These processes are referred to as network layers [J. Wu, 2017]. Convolution begins with implementing a kernel to a portion of the element (typically a 2 x 2 or 3 x 3 matrix as a filter). This is usually the location of its first-pixel resolution on the upper left portion of the digital image that fits the kernel size. Figure 4.5 shows how to compute the first-pixel value in a Feature map with a 6 x 6 input image and a kernel size of 3 x 3. The new feature value set determines all values by employing Eqn. (4.8).

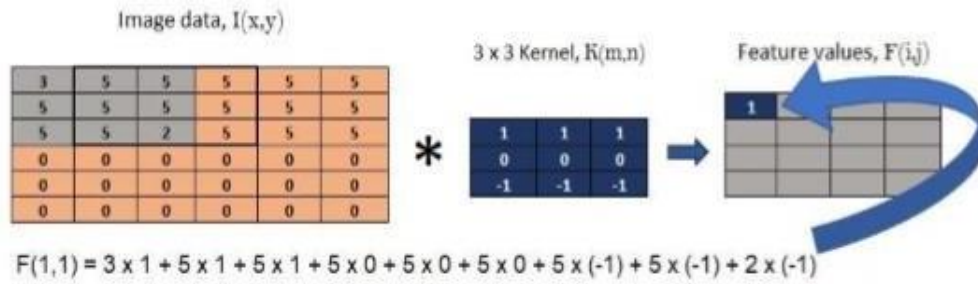


Figure 4.5 Extraction of CNN feature values [Reproduced by I. Mebsout, 2020]

This kernel is moved in 1-step intervals from left to right on image data. Strides are the unit of measurement for these step increments. This convolution has a stride value of 1. The following equation represents the convolution F of a kernel and picture data [P. Skalski, 2019].

$$(i,j) = \sum \sum (m,) \cdot (i - m, j - n) \quad (4.8)$$

Where I is the input image in I and j dimensions, K is the $m \times n$ -dimensional kernel, and $F(I,j)$ is the throughput fully connected layers matrix. Many Neural network models include activation functions, pooling layers, fully connected layers, dropout, flatten, and output layers. For this research work, all of the previously stated layers were available in numerous layouts in CNN models.

4.4.2 Activation Function

An activation function typically follows each Convolution layer in a convolution neural network model. The Rectified Linear Unit function (ReLU) is a popular choice for most Convolutional networks. ReLU sets the negative input parameters feature matrix to zero [U. Ujjwalkarn, 2016]. Because Convolutional neural networks are primarily used for actual data processing, the learning model must be nonlinear, as convolution is a linear operation [U. Ujjwalkarn, 2016]. ReLU is mathematically given in Eqn. (4.9).

$$f(x) = \max(0, x) \quad (4.9)$$

For any negative entries of input x , the above equation computes ReLU, $f(x)$ to generate zero output values and identity otherwise. Rectified Linear Unit Activation Function (ReLU) is shown in Figure 4.6.

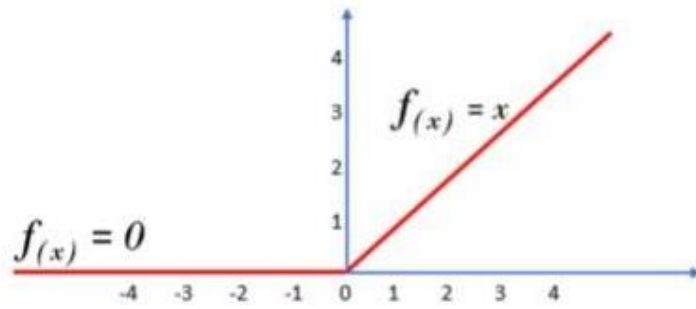


Figure 4.6 Rectified Linear Unit Activation Function (ReLU) [Reproduced by I. Mebsout, 2020]

4.4.3 Pooling Layers

After convolution layers in CNN, pooling coatings reduce the spatial dimensions of feature maps, likely to result in a matrix with lower dimensionality and more meaningful characteristics. Figure 4.5 to Figure 4.8 explain how to convert a 4×4 matrix to a 2×2 feature value set. Pooling layers aid in reducing the number of network parameters, which helps to avoid over fitting issues. In convolution neural network models, over fitting occurs when the neural network is trained on original detailed information and noise input, resulting in a negative classification effect [J. Brownlee, 2016].

The operation is chosen for pooling steps, and a 2×2 window is employed in the same way as in Figure 4.7. In this case, the peak of each set is chosen as an attribute input for the attribute value system.

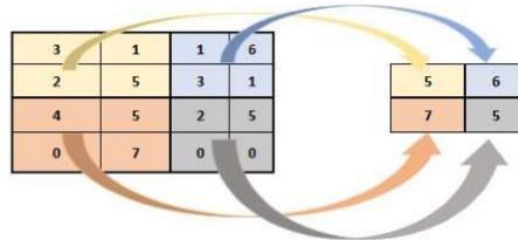


Figure 4.7 Max pooling on convolution layer [Reproduced by I. Mebsout, 2020]

4.4.4 Soft-max activation and fully interconnected layer

A subset of features with one of the most meaningful data obtained from convolution and pooling layers is used in fully connected coatings, where each node (receptors in a neural network) over the successive layers is attached to neurons in the following levels. Dense layers refer to layers that are fully connected. Fully linked layers use the retrieved attributes from previous layers to conduct initial classification on the training dataset [U. Ujjwalkarn, 2016]. The thoroughly combined and softmax layers in CNN's architecture are shown in Figure 4.8. Finally, the training data classes are classified using the Softmax activation layer.

4.4.5 Dropout and Flatten Layers

Dropout layers are employed before the output layer to remove some data from specific network neurons to prevent overfitting [N. Srivastava et al., 2014], whereas flattened layers are used before the output layer to transform the multidimensional output into a vector [N. Srivastava et.al, 2014][J. Brownlee, 2016]. This phase is needed to determine the throughput structure depending on the number of classes learned and forecasted. For example, if the required information for a Convolutional neural network training session were divided into two classifications, the flattened layer would be necessary to minimize the outcome of the fully connected layer to a single category: two vectors, each one of the categories. A significantly bigger vector is formed at the output layer for more attribute information classification.

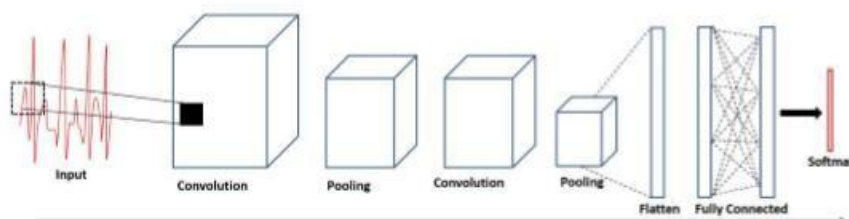


Figure 4.8 A complete Convolutional neural network sequence with fully connected and soft-max strands for output [Reproduced by I. Mebsout, 2020]

4.4.6 Literature Survey of Classification of Arrhythmias

This chapter summarizes a few of the earlier strategies for identifying irregular heartbeat in ECG signals. Because this research focuses on utilizing neural networks for classification, the literature study was confined to machine learning and deep learning approaches. [S. Sahoo et.al., 2020] comprehensively analyzed various machine learning approaches used for ECG analysis and arrhythmia diagnosis. The parts in this chapter cover some of those strategies in greater depth. In addition, at the end of this chapter, a brief explanation of transfer learning via CNN is included.

As explained in the previous chapter, preprocessing is a necessary step to implement after acquiring ECG records due to the signal's noise [A. Isin. and S. Ozdalili, 2017]. One of the major impacts is the reduction of dc (direct current voltage) noise from the Electrocardiogram signal called preprocessing [A. Isin. and S. Ozdalili, 2017]. The mean subtraction method can be used to accomplish this. Moving average filters can also be employed to eliminate high-frequency noise. Low-frequency noise can be removed using high-pass filters. Bandpass filtering was used to remove power line noise, according to [A. Isin. and S. Ozdalili, 2017]. In the proposed work, deep-learned CNN is applied to the network for classification, which utilizes the fully connected layer to classify signals. As a result, we investigated the model's optimized results using different kinds of classifiers.

4.4.7 Deep Convolutional Neural Network (DCNN)

The author suggested a deep convolution neural network for noised or noise-free ECG signals for arrhythmia identification. The detection of time-associated information order of ECG heartbeat signal was a shortcoming of this method. Another technique the author employs is the support vector machine, in which the classifier's output is optimally set for maximum classification output. The downsides of this strategy include the fact that classification takes long. Knowledge is gathered from several sources in the knowledge base technique. Artificial intelligence assists in the resolution of challenges and complex issues (AI). The disadvantage of this strategy is that it needs to take into account ineffective beat labelling. [T. Teijeiro, P. Felix et.al, 2018].

4.4.8 Genetic algorithm-based back-propagation neural network (GA-BPNN)

A hybrid model integrating a genetic algorithm and a back-propagation neural network (GA- BPNN) was employed to improve forecast performance. However, when dealing with a big neural network, a standard genetic algorithm might readily slip into local optimization problems and local connectivity. An improved genetic algorithm is proposed to address this challenge, coupling a back-propagation neural network model (IGA-BPNN) with various genetic techniques. Among the strategies are:

- A chaotic sequence.
- Multi-type genetic strategies.
- Adaptive dynamic probability adjustment.
- An attenuated genetic approach.

The authors' technology, a genetic algorithm-based back-propagation neural network (GA-BPNN), provides an efficient and feasible technique for diagnosing/detecting critical faults. This strategy has the disadvantage of not delivering real-time data between modules.

4.4.9 CNN+LSTM

CNNs, also referred to as feature learners, have a lot of potential for extracting meaningful features from raw data. CNNs generally have two components, each serving a distinct purpose. The feature extractor is the first section of a CNN and is in charge of extracting features automatically. The second component is the fully connected multi-layer perceptron (MLP) classifier. The entire system is connected. The pooling layer is one of the most prevalent subparts in the feature extraction section. Max, Min, and Average pooling are three different types of pooling layers. The feature maps' resolution can be reduced by using a pooling layer. The suggested model uses the max-pooling operation to find the most significant value in neighboring inputs [J. K and C.Y.M. Zubair, 2016]. In terms of complexity, there is a distinction between the two sections. Compared to the completely connected layers, the principal layer's feature extraction component performs more computations, including feature extraction and feature selection [Z. Zhang et al., 2014]. Many similarities exist between the CNN and ANN structures with input, hidden, and output layers. Convolution neural network (CNN) is an updated version of the artificial neural

network that, unlike NN, is both translational and shift invariant. In most cases, CNNs are composed of multiple layers, including input, convolution, max pooling, average pooling, drop layer, and Softmax layer, and each plays a different function in the model [F. Elha, N. Salim et.al, 2016].

Medical practitioners and cardiologists frequently employ ECG analysis to assess cardiac health. In a high-performance automatic ECG classification system, detecting and clustering multiple waveforms in the signal is difficult, particularly in evaluating electrocardiogram (ECG) signals. In this research work, the implementation of 1D Convolutional Neural Networks (CNNs) and Long Short-Term Memory is used to suggest an exact (ECG) classification and monitoring system (LSTM). The CNN model captures the learned characteristics, subsequently supplied to the LSTM model. The following technique is a combination of convolutional neural network and long short-term memory; in this technique, authors proposed a model which is the hybrid of convolutional neural network (CNN) and long short-term memory (LSTM) for the detection of classification of several cardiac rhythms. The main benefit of this technique was the accuracy of screening ECG. The drawback of this technique was the detection and recognition of variation of periods in long and short signals of heartbeat.

Another methodology the authors offer is the convolution neural network (CNN), which is very beneficial for detection and does not necessitate any feature extraction or assistance from an expert. The disadvantage of this method is that it needs to address resilience in long-term applications.

4.4.10 BaROA DCNN classifier

The suggested BaROA algorithm combines the MOBA and the ROA in such a way that the update rule of the bypass rider is modified using the update equation of ROA. The suggested BaROA algorithm balances the advantages and disadvantages of MOBA and ROA and works significantly; it has a higher rate of convergence with the best solution and a stronger preference for the best solution avoidance technique. On the other side, better convergence rates ensure that the solutions are diverse and BaROA's capacity to cope with numerous objectives is effective. ROA is generally based on theoretical concepts and employs a novel computing environment known as fictional computing, which is distinct from artificial computer technology and

environment platforms. ROA is determined by the optimization features of the riders, which are divided into four categories: bypass, overtake, attacker, and observer.

Each rider has their personality and wants to get to their destination. The success rate determines the best rider, which should be as high as possible for the top or leading rider. In addition, it is essential to remember that ROA is the sole optimization in the hypothetical perspective. The most crucial aspect of ROA is that it renders the global optimal solution, which is nothing more than the classifier's weights and biases. Furthermore, the positions of the other four groups of riders are updated based on the leading cyclist's position, and the parameters required for upgrading the roles also include steering angle, activator, gear, and so on.

The author's following technique is the BaROA DCNN classifier, an improved version of the BaROA in a deep Convolutional neural network (CNN). This strategy uses the enhanced version of ROA to determine the updated weights of the classifier's target and the multi-objective bat algorithm (MOBA). Due to the minimal features collected from the electrocardiogram (ECG) data, this classifier is highly accurate.

4.4.11 Proposed Work

The proposed approach for securing the ECG signal during transmission is described in this section. Figure 4.9 shows the suggested method's block diagram of the proposed work. This approach obtains data from the MIT-BIH database, which is subsequently down-sampled. [N. Raheja and A.K. Manocha, 2021]. To remove artifacts from the electrocardiogram (ECG) signal and to achieve a better output, the sampled signal is given to Savitzky-Golay (SG). A wavelet transform called the Maximal overlap wavelet packet transform is employed to reduce high-frequency artifacts. After removing the noises present in ECG, signal characteristics are retrieved using the wavelet transform, and the number of features is provided before the message is transmitted to the network, which is used as input to classifier and the provided to an encryption authentication mechanism for security.

The information is then encrypted in the second step using the triple data encryption standard (3-DES) algorithm in cipher-block-chaining (CBC) mode. This method transmits encrypted data and a verification tag that allows the receiver to confirm the data's authenticity. Three data encryption inputs are required for the CBC mode:

hidden information, security key, and IV key. As a result, the water cycle optimization (WCO) technique is used to obtain the IV key. Then, specified blocks are created from the digitized ECG data (64 bits). The triple data encryption standard (3-DES) technique encrypts the block data information and initializes the vector key (IV) and security key. The first frame's encrypted data is the event data initialize vector (IV) key. The encryption procedure must be repeated for each block to obtain encrypted data in the output.

In addition, the encrypted data in the last block serves as an authentication label, enabling the receiver to verify the validity of the data. Various security metrics are used to evaluate the performance of data encryption. ThingSpeak uploads encrypted information and authorization tags to the cloud in the third step. The personal and initialization keys are also sent to the receiver across a secure channel. A flow diagram of data decryption on the receiver side is shown in Figure 4.10 and Figure 4.11. The receiver downloads the encrypted information and the verification tag from the cloud. The user key and initialization vector (IV) key are also retrieved similarly through the secure communication channel. The encrypted data, user key, and IV key are sent to the decryption process, which outputs the secret data. The authentication tags are contrasted after that. The authentication was successful if all the authentication tags contained the same value; else, it failed. A message telling the transmitter to retransmit the information is delivered if the data is false; otherwise, post-processing is done to receive the electrocardiogram (Electrocardiograph) signal.

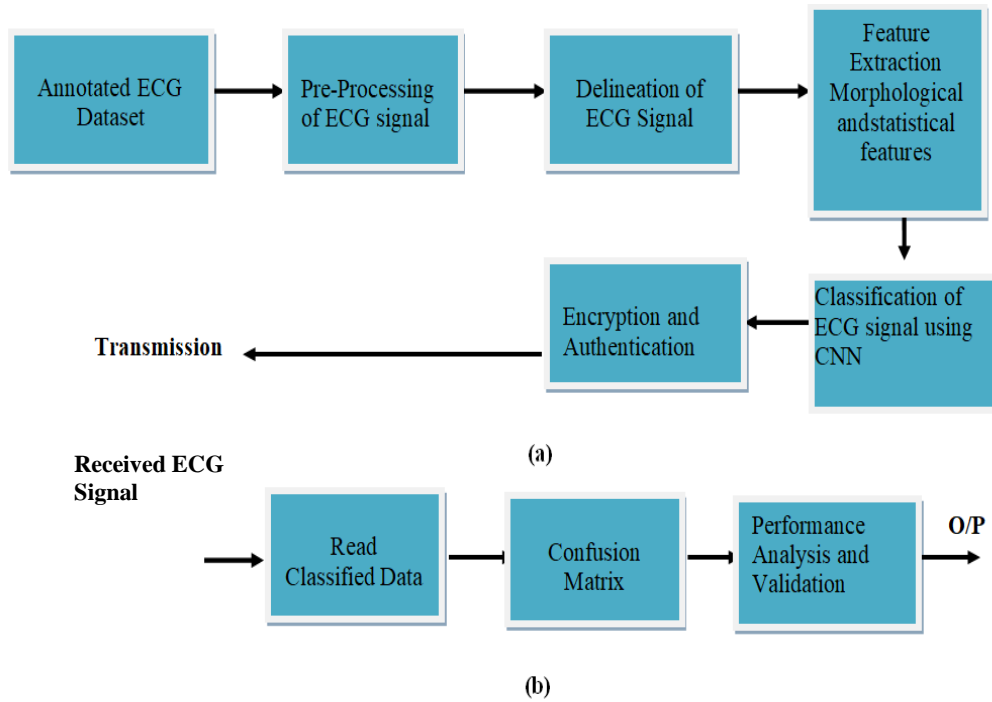


Figure 4.9 Block diagram of proposed research work (a)Transmission of ECG using Thingspeak cloud (b) Receiver

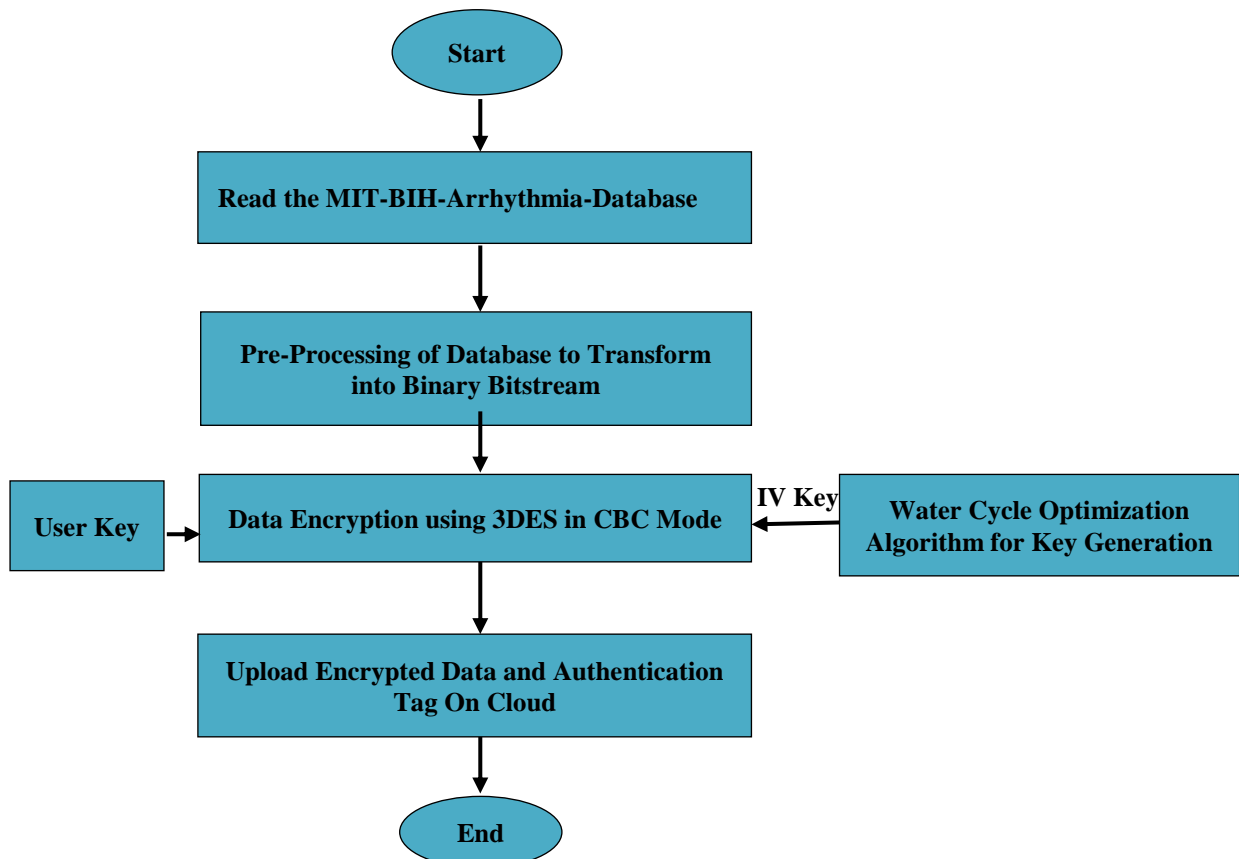


Figure 4.10 Proposed Data Encryption at Transmitting End Security Mechanism

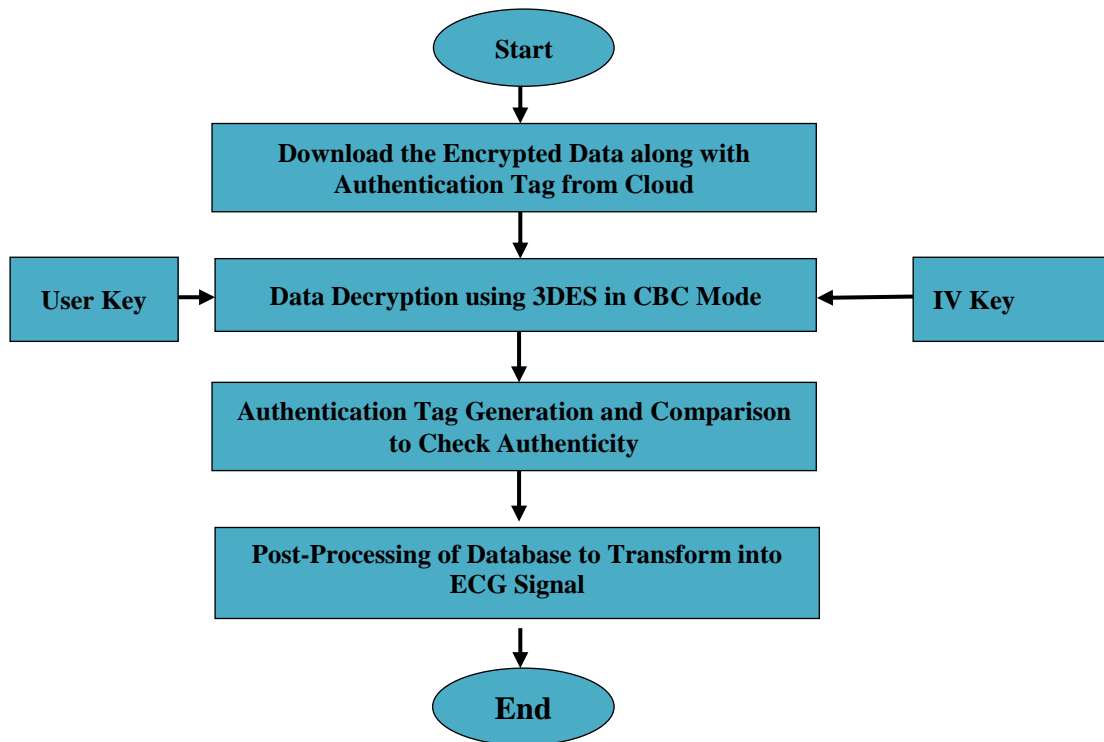


Figure 4.11 Data Ciphering and Verification Proposed Method at the Receiver End

Because ECG signals are millivolt signals, they are extremely sensitive. As a result, maintaining critical information in an electrocardiogram and transmitting electrocardiogram. (ECG) Reporting to a specialist is one of the most pressing issues in the medical system. This program aims to produce a one-time encryption key that authenticates and encrypts information to guarantee secrecy and authenticity. In transmitting information for electrocardiograms, symmetric encryption methodologies are favored over asymmetrical key techniques.

In the literature, there are numerous encryption algorithms such as Advanced Encryption Standard (AES), data encryption standard (DES), Triple data encryption (3-DES), Blowfish, Rivest–Shamir–Adleman (RSA), Two fish, and so on. In contrast, Triple data encryption (3-DES) reduces Processor and storage use [V. Goyal and A. Zafar, 2020] [G. Singh and Supriya, 2013]. Furthermore, AES is more suitable for the triple-data encryption standard, created for hardware implementations only. In a similar vein, 3-DES is appropriate and compatible with IoT devices. The Electrocardiogram subsystem for IoT systems employs the Low - power wireless protocol, which is typically limited in area and electricity. Compared to AES- based techniques, the triple data encryption standard requires significant RAM and energy.

It is not suitable for portable alternatives (like IoT systems). We selected the triple data encryption standard as IoT encryption in the proposed approach, but AES should be investigated further. The Security and authentication strategies were employed to guarantee the accuracy of the data. An experiment was conducted based on standard ECG signals, and many results were found. The confidentiality and statistical public key tests in this work have been enhanced using this method. Figure 4.12 depicts the workflow for the data encryption technique that has been proposed. Use the XOR algorithm to combine the cipher and the initiation vector (IV) key first.

The XOR output was then fed into the encryption system, which produced the cipher text and the secret key in the production. The cipher text was created by repeating the process with the remaining text data. The plaintext block also serves as an authenticity tag, protecting the security of the system's content. The steps in the suggested method are as follows:

Generalized Steps in the Encryption Process

- Step-1 Secured data and secret keys are input.
- Step-2 Data encryption and authentication tag are the outputs.
- Step-3 Read the confidential documents and split them into 64-bit frames.
- Step-4 Examine the secret code.
- Step-5 Using the water cycle approach, generate the initialization vector key (IV).
- Step-6 For block ciphers, a private data frame, private keys, and initialization vector key are provided to the 3-DES algorithm.
- Step-7 The encrypted data then serves as an Initialization Vector (IV) key for the following block.
- Step-8 Repeat steps 3–4 until all of the confidential data has been encrypted.

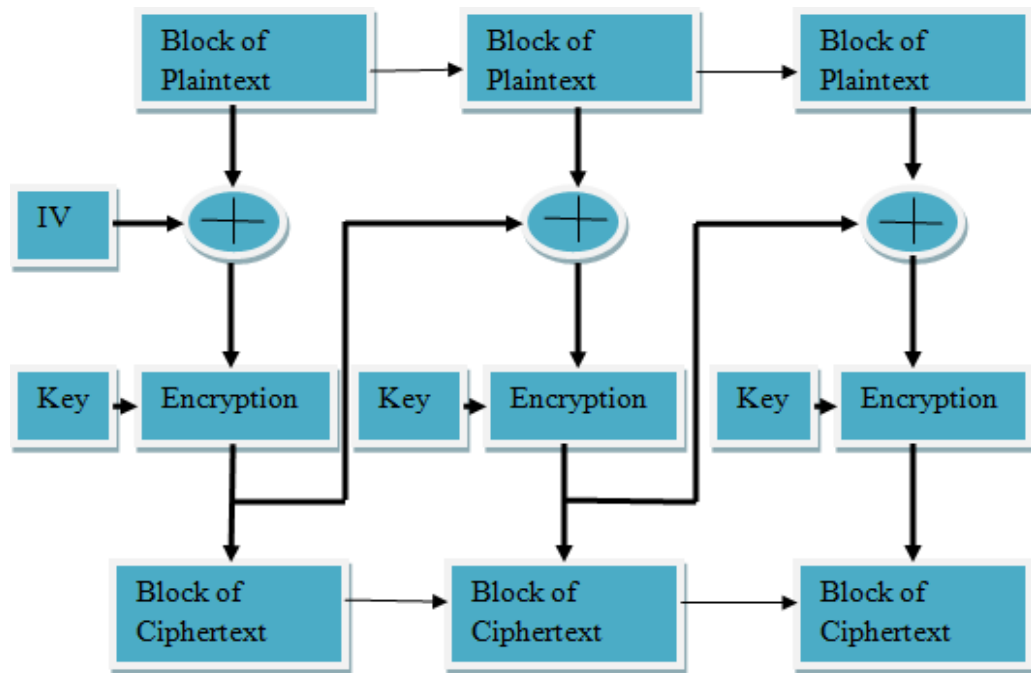


Figure 4.12 Flow diagram of the presented data encryption algorithm

[Reproduced by V. Goyal and A. Zafar, 2020]

4.5 Proposed Water Cycle Optimization Process (WCO)

[A. Barzegar et al., 2019) describe it as the primary stream and river workflow implementation using a meta-heuristic optimal technique. Create an arbitrarily defined river or scheme factor population in the range between the higher and lower limitations to start a precipitation or rainfall approach in this procedure. Figure 4.13 depicts the WCO flow diagram [H. Eskandar et al., 2012].

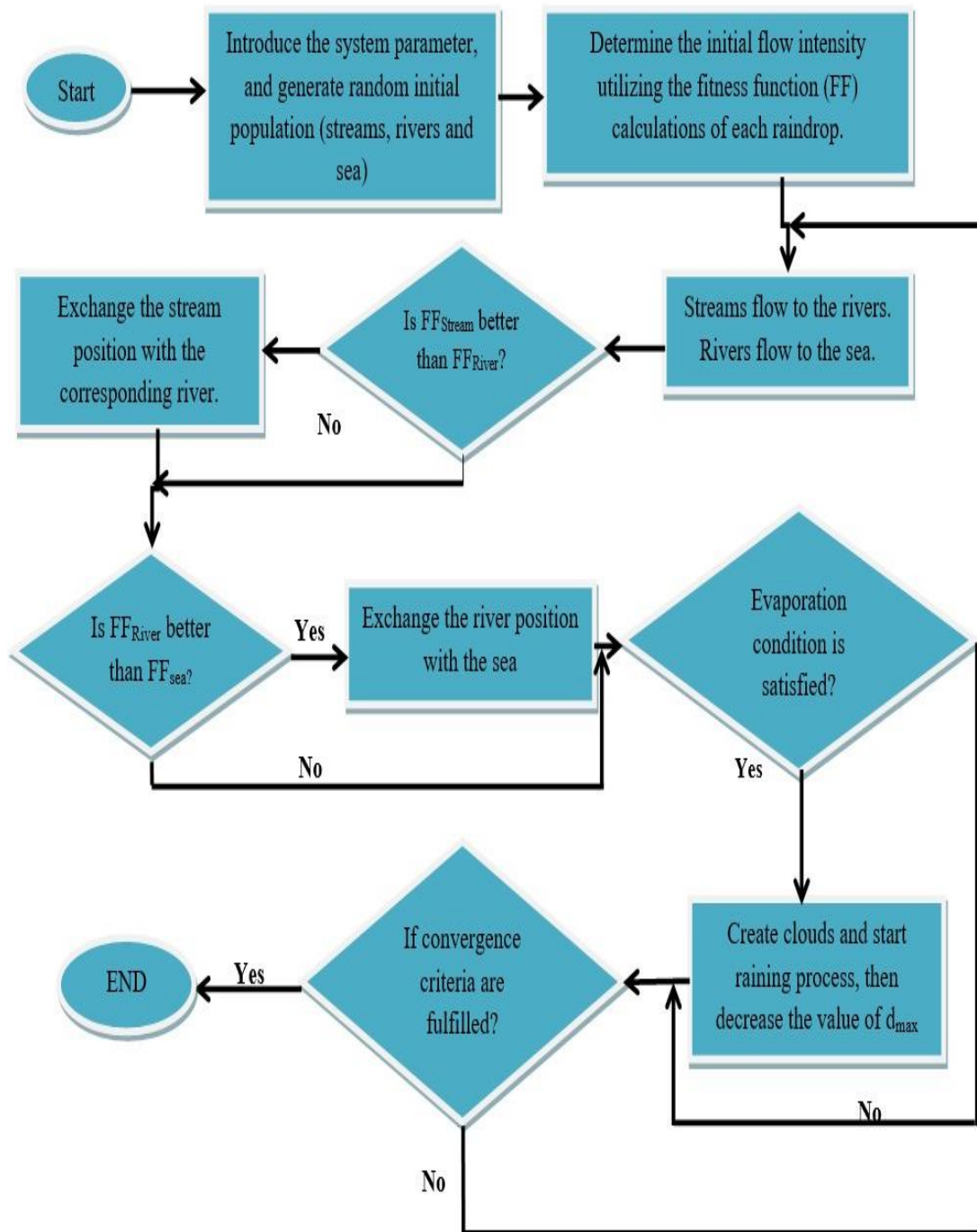


Figure 4.13 Flow diagram of water cycle optimization [Reproduced by H. Eskandar et al, 2012].

The best optimal flow is chosen for the problem minimization, with the stream acting as the sea and the valuation of the very most minor target function. The number of river classes selected from the river is based on its target value. Eqn. (4.10) represents the mathematical representation of the water cycle algorithm. Let's have a look at the potential solution, which is a 1-D array (i.e., the flow).

$$X = [x_1, x_2, x_3, \dots \dots x_D] \quad (4.10)$$

Where 'D' denotes a design, variable used to initialize the procedure. Suppose consider an individual indicated by Npop*D and calculated using Eqn. (4.11).

$$\begin{aligned} \text{Total Population} &= \begin{bmatrix} \text{Sea} \\ \text{River}_1 \\ \text{River}_2 \\ \text{River}_3 \\ \vdots \\ \vdots \\ \vdots \\ \text{Stream}_{Nsr+1} \\ \text{Stream}_{Nsr+2} \\ \vdots \\ \vdots \\ \text{Stream}_{Npop} \end{bmatrix} \\ &= \begin{bmatrix} x_1^1 & x_2^1 & x_3^1 & \dots & \dots & \dots & \dots & x_D^1 \\ x_1^2 & x_2^2 & x_3^2 & \dots & \dots & \dots & \dots & x_D^2 \\ \vdots & \vdots & \vdots & \vdots & \vdots & \vdots & \vdots & \vdots \\ x_1^{Npop} & x_2^{Npop} & x_3^{Npop} & \dots & \dots & \dots & \dots & x_D^{Npop} \end{bmatrix} \end{aligned} \quad (4.11)$$

The N_{pop} represents the population size. To take into account the stream and the ocean, you must first determine the population that will arise from each river's cost value. To get each stream's cost value, X_i considers the cost value for that flow as indicated in Eqn. (4.12).

$$.C_i = Cost_i = f(x_1^i, x_2^i, \dots \dots, x_D^i) \quad i = 1, 2, 3, \dots \dots, N_{pop} \quad (4.12)$$

The client's boundary is known as N_{sr} , which is utilized to select the river and sea quantity, according to Eqns. (4.13) and (4.14) calculations, the individuals with the lowest values are referred to as the sea, and different sequences (flow) are chosen as the stream.

$$N_{sr} = \text{Number of Rivers} + 1 \quad (4.13)$$

$$N_{stream} = N_{pop} - N_{sr} \quad (4.14)$$

As a result, the equation provides the individuals of the stream that is assigned to the river and the sea given in Eqn. (4.15)

$$\begin{aligned}
\text{Population of Streams} &= \begin{bmatrix} \text{Stream}_1 \\ \text{Stream}_2 \\ \vdots \\ \vdots \\ \vdots \\ \vdots \\ \vdots \\ \vdots \\ \vdots \\ \text{Stream}_{N_{\text{stream}}} \end{bmatrix} \\
&= \begin{bmatrix} x_1^1 & x_2^1 & x_3^1 & \dots & \dots & \dots & \dots & \dots & x_D^1 \\ x_1^2 & x_2^2 & x_3^2 & \dots & \dots & \dots & \dots & \dots & x_D^2 \\ \vdots & \vdots & \vdots & \vdots & \vdots & \vdots & \vdots & \vdots & \vdots \\ x_1^{N_{\text{stream}}} & x_2^{N_{\text{stream}}} & x_3^{N_{\text{stream}}} & \dots & \dots & \dots & \dots & \dots & x_D^{N_{\text{stream}}} \end{bmatrix}
\end{aligned} \tag{4.15}$$

Where N_{stream} is the proportion of the total population, all the seas and rivers use a significant amount of water from their streams. The flow of water into a river or ocean is measured by measuring the flow in specific streams that run directly into the sea. Because all river water goes into the deepest sea, the intensity of flow is estimated by Eqns. (4.15) and (4.16) are used to compute the stream water flows into rivers and seas:

$$C_n = \text{Cost}_n - \text{Cost}_{N_{\text{sr}}+1} \tag{4.15}$$

Where $n = 1, 2, 3, \dots, N_{\text{sr}}$

$$N_{S_n} = \text{Round} \left\{ \left| \frac{C_n}{\sum_{n=1}^{N_{\text{sr}}} C_n} \right| \times N_{\text{stream}} \right\} \quad n = 1, 2, 3 \dots N_{\text{sr}} \tag{4.16}$$

Where N_{sr} is the number of rivers and N_{S_n} the current of streams that flows into the particular river or sea and N_{s1} is the amount of water flowing into the ocean, and N_{s2} is the amount of water that flows into the river. In nature, it is considered that rainfall and precipitation make the rivers which are formed by connecting the number of rivers. Some stream flows directly into the sea. Even all the streams and rivers flow into the sea. This is the ideal optimal achievement. Figure 4.14 depicts the flow of a stream to a river, with a line connecting them using an arbitrarily chosen distance given by Eqn. (4.17)

$$X \in (0, C \times d), \quad C > 1 \tag{4.17}$$

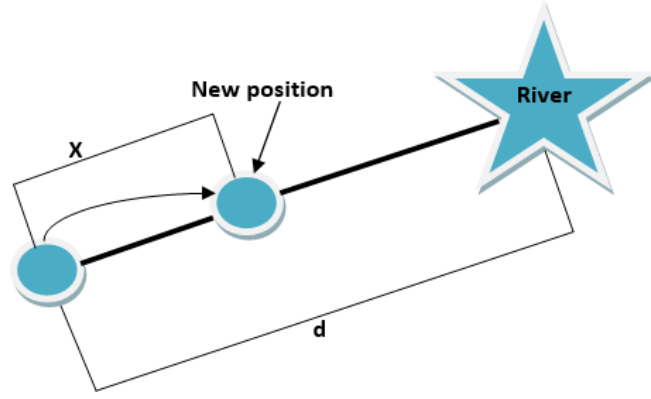


Figure 4.14 Stream flow into a certain river (circle and star address the stream and river individually) [Reproduced from A. Barzegar et.al, 2019]

Where the value of 'C' is in the range of 1 to 2. The best option is to choose 2 as the best value. The 'd' specifies the spacing between the stream and the river. 'X' can have values ranging from 0 to (c*d). The value of c must be higher than one for the stream to enter the rivers from multiple directions. The movement of a river to the sea follows a similar principle. Eqns. (4.18) and (4.19) are used to calculate the new position of the stream and river.

$$x_{stream}^{i+1} = x_{stream}^i + \text{rand} \times C \times (x_{river}^i - x_{stream}^i) \quad (4.18)$$

$$x_{river}^{i+1} = x_{river}^i + \text{rand} \times C \times (x_{sea}^i - x_{river}^i) \quad (4.19)$$

Where 'rand' denotes a random number between 0 and 1. If the stream's calculated answer is better than the river's, the stream and river's positions are swapped. Rivers and the sea can also be replaced in this way. Figure 4.15 depicts the stream replacement, which is the finest and most optimized solution among the streams and rivers.

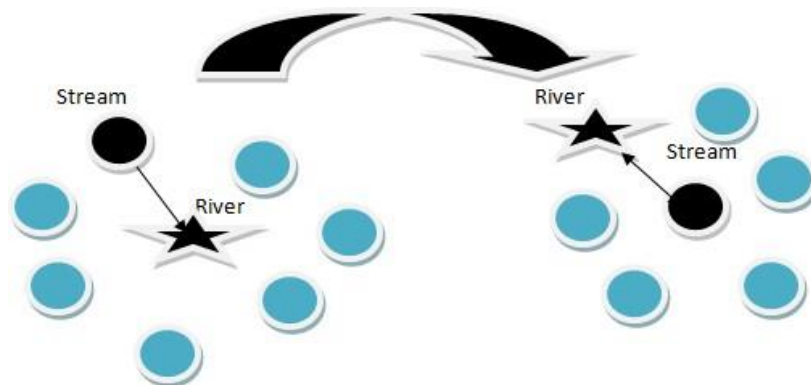


Figure 4.15 Replacing the streams and the river regions (where the star used here for the river and the black color circle used to represent the best stream between all other streams) [Reproduced from A. Barzegar et.al, 2019]

4.5.1 Evaporation Condition

One of the most essential considerations in protecting the repaid immature convergence is this. Water evaporates from lakes and rivers, just as it does in nature, whereas Plants, on the other hand, produce water during photosynthesis. Evaporation carries moisture in the atmosphere, leading to the development of clouds, which leads to a cooler climate and the development of rain. In this way, liquid returns to the ground. Rain forms a new stream, flowing into rivers and the sea [S. David, 1993]. As a result, this procedure is known as water cycle optimization. In this approach, evaporation drains away sea water as streams or rivers move to the sea. This procedure was used to prevent the local optimal value obtained using Eqn. (4.20).

$$\text{If } |x_{sea}^i - x_{river}^i| < d_{max} \quad (4.20)$$

Where $i=1,2,3, \dots, N_{sr}-1$

' d_{max} ' has a minimal value close to 0. If the distance between the river and the sea is less than d_{max} , the river and the sea have merged. The condensation process was used in this case and the rainy procedure will begin after some suitable evaporation. As a result, d_{max} directs the search for the best solution. As seen in Eqn. (4.21), the value of d_{max} decreases adaptively:

$$d_{max}^{i+1} = d_{max}^i - \frac{d_{max}^i}{\text{max iteration}} \quad (4.21)$$

4.5.2 Raining Process

The raining process was used after the evaporation procedure had been completed. New droplets emerged from the stream at various spots during this process. The equation indicates the new position in the freshly generated stream Eqn. (4.22).

$$X_{stream}^{new} = LB + \text{rand} \times (UB - LB) \quad (4.22)$$

The issues determine where 'LB' denotes the lower band and 'UB' means the upper band. Similarly, the fresh raindrop's development is likened to a river flowing into the sea. The remaining droplets will create a new stream flowing into the river or directly into the sea. The rate of convergence and the acceleration of algorithmic throughput of only streams that come directly into the sea use the algorithm for the confined problem described in Eqn. (4.23). To improve the optimum value, the goal of this equation is to encourage the creation of a stream that runs into the sea.

$$X_{stream}^{new} = X_{sea} + \sqrt{\mu} \times \text{randn}(1, N_{var}) \quad (4.23)$$

Where μ is a co-efficient which indicates the range of region close to the sea, rand_n is a random number that is normally distributed. As the value of μ is large, then the possibility of exit from the feasible reason increases. Similarly, as the value of μ is small, then the algorithm starts to search for the smaller value near the sea. Here $\sqrt{\mu}$ represents the standard deviation and the value μ is considered as 0.1.

4.5.3 Handling Constraints

In this method, the stream and rivers criticize the particular restrictions and difficulties or govern the system parameters. In this presented research, the best optimal solution method is used to solve problems, which is summarized in the following solution [E.M. Montes and C.A.C. Coello, 2008].

- Step 1: Any feasible solution can be used to solve an infeasible challenge.
- Step 2: The most useful strategy for the infeasible problem is a minor traffic violation of the boundaries.
- Step 3: The solution with the superior objective function is chosen from the two options.
- Step 4: The solution with the lowest boundary infringement valuation is chosen between the two infeasible solutions.

The search for a feasible solution is carried out using the first and fourth steps. After that, the third step was used to find the best possible option. Step 2 allows the stream and rivers to reach the borders and, with high probability values, approach the global minimum.

4.5.4 Criteria for Convergence

The best option is then evaluated using optimization techniques, such as the number of epochs and CPU time frames (or), and it is a very short and mid score. The sensitivity valuation is then calculated by contrasting the results of the final two procedures. The water cycle optimization method is executed until the number of iterations necessary to satisfy the completion requirement is attained. Figure 4.16 shows the water cycle algorithm (WCA) procedure. Diamonds, stars, and circles symbolize the sea, river, and stream. The shaded circle and stars represent the river and its current location, while the black circle shows the river's historical position.

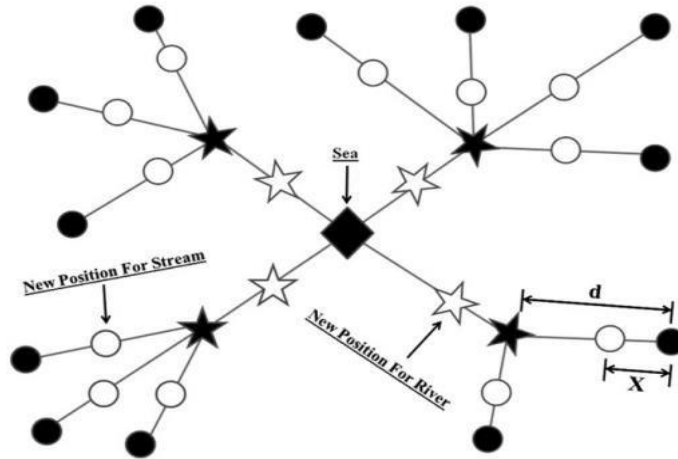


Figure 4.16 Procedure of water cycle algorithm (WCA) [Reproduced from A. Barzegar et.al, 2019]

4.6 The Proposed Triple Data Encryption Standard (3-DES)

In this research work, we have proposed the triple DES algorithm that performs the implementation of the algorithm three times. Data encryption standard (DES) employs 56- bits of the key, which is insufficient for encrypting sensitive data [Z. Yang et al., 2016]. Whereas triple DES uses the keys, which expand the size of the key used in DES. TDEA utilized three 64-bit keys (K1, K2, K3). After combining the entire key, the size is 168- bits (3 times the 56) in encryption-decryption-encryption (EDE) mode, as shown in Figure 4.17. When using encryption-decryption-encryption (EDE), the size of the entire key after it is combined is 168 bits (3 times the 56) given in Eqn. (4.24).

$$C = E(K3, D(K2, E(K1, P))) \quad (4.24)$$

Here are some examples of how to use three different keys:

- The first three keys (K1, K2, and K3) are used because they are mutually independent. It generates keys of $3 \times 56 = 168$ bits in length.
- The pair of keys are also used separately, along with a third key that is the exact same as the first ($K1 = K2$ and $K3 = K1$).
- Finally, use the three corresponding keys ($K1 = K2 = K3$). This phase corresponds to the data encryption standard algorithm. Iteration three times is used in triple DES to enhance the strength of cryptography and the mean duration of information.

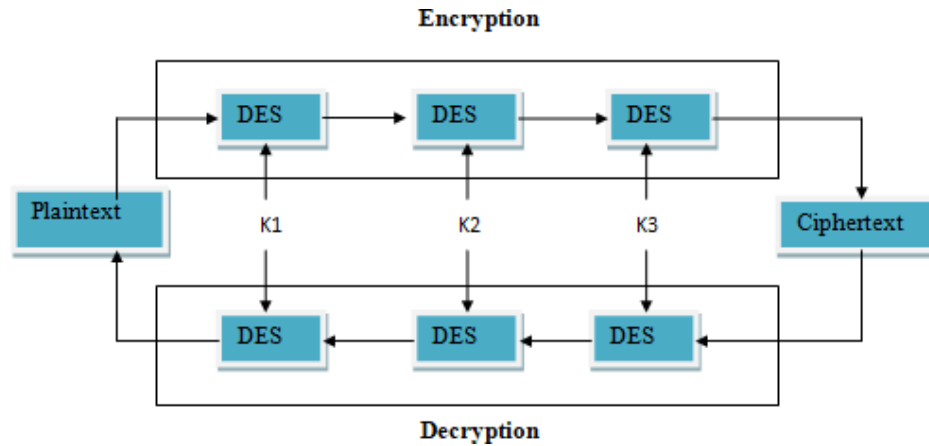


Figure 4.17 Encryption and Decryption of Triple-DES [Reproduced from O. S. Rao, 2015].

4.7 The proposed ThingSpeak IOT Platform

The proposed methodology involves teleconsultation, tele-echocardiography, tele-ECG and e-teaching to provide a superior choice. It allows the sharing of patient information in real time domain as well as analysis of ECG data. The Internet of Things (IoT) offers a framework for connecting medical equipment that may collect, analyse, and sharing data as well as connection to specialists and store data in the cloud or on servers. Systems for health and wellness operated by the internet of things (IoT) enable remote and continuous monitoring of patients with chronic diseases [A.K. Sangaiah et al., 2020]. Increasing the ease of access to are, making it more affordable, and dramatically reducing travel and therapy expenses will significantly contribute to enhancing IoT health and welfare. The Internet of Things (IoT) is used in the IoT-based healthcare system to connect biosensors and prototype, which acquire a variety of biomedical signals and use interoperability to communicate the signals immediately with the internet and health professionals as shown in Figure. 4.18 and 4.19. The building of the proposed work on the IoT (Internet of medical thing) is shown in Figure. 4.20. Additionally, long-term monitoring applications that are permitted by IoT can be significantly more cost-effective, time-efficient, and travel-efficient [S. Kumari et.al, 2018]. In presented research work, we have used MIT-BIH recordings instead of real time acquisition of ECG signals. The Internet of Things (IoT), open-source platform is used i.e., ThingSpeak for the detection and identification of cardiac arrhythmia process on the cloud channel to monitor the cardiac disease [A.K. Sangaiah et al., 2020]. ThingSpeak is an internet of thing peripheral interference application for processing, storing, and receiving ECG data

over the internet and via LAN (Local area network) [S. Kumari et.al, 2018]. This platform permits visualization and analyses of the live data stream in the cloud.

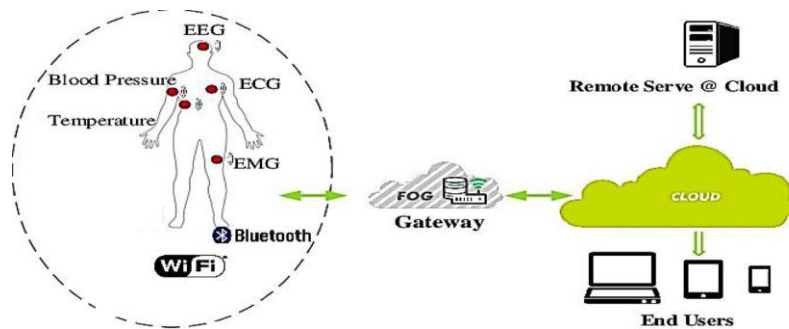


Figure 4.18 Framework for IoT-enabled Electrocardiography [Reproduced by A.K. Sangaiah et al., 2020]

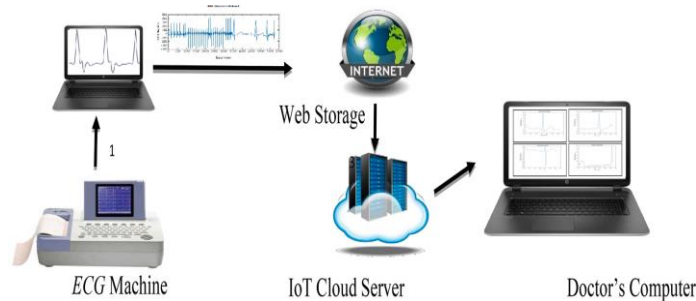


Figure 4.19 Prototype of the proposed work [Reproduced by A.K. Sangaiah et al., 2020]

4.7.1 Architecture of Internet of Things (IoT) technique

The Internet of Things (IoT) open-source platform ThingSpeak is used in this proposed effort to detect and identify cardiac arrhythmia processes on the cloud platform to monitor cardiac illness. ThingSpeak is a peripheral interference Internet of Things program for processing, storing, and receiving ECG data through the Internet and LAN (local area network) [A.K. Sangaiah et al., 2020]. This stage permits clients to see and analyses real-time data streams in the cloud. Figure 4.18 depicts the construction of the proposed work on the IoMT (Internet of medical things).

In this proposed study, heart arrhythmia processes are detected and identified on a cloud platform using the open Platform of Things (IoT) platform ThingSpeak. A peripheral interference IoT (Internet of Things) software called ThingSpeak allows users to analyze, preserve, and retrieve ECG data over LAN and the Internet [A.K. Sangaiah et al., 2019]. This stage permits clients to see and analyses real-time data streams in the cloud. Figure 4.19 shows how the suggested Internet of Things project

would be built and Figure 4.20 shows the architecture of proposed IoT approach. The MATLAB and stabilizer tools are combined in the ThingSpeak Internet of Things. A real-time line-up of the given detection and treatment of heart arrhythmia is accomplished using the Internet of Things (IoT) technique.

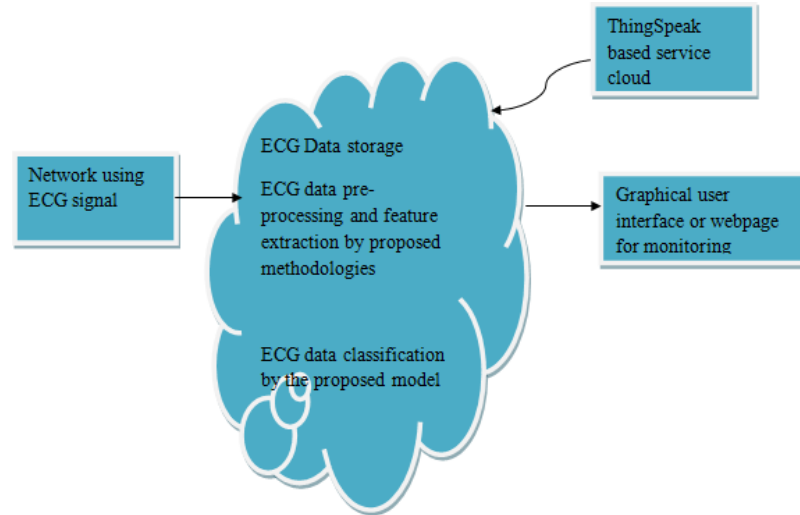


Figure 4.20 Architecture of proposed IoT approach [Reproduced from A.K. Sangaiah et.al, 2019]

In the IoT framework, in light of the Electrocardiogram module, the Bluetooth low energy methodology is used to communicate the monitoring of patient's information progressively to a phone or tablet running the Android working framework. Not only are tablets and smartphones used to operate the ECG modules which show ECG information, but they likewise communicate ECG information to a server via the web. This server is used to access or store ECG data [S. Kumari et.al, 2018]. As seen in Figure 4.21, there are two stages to the data transfer method. The purpose of connecting Bluetooth in the first step is to create a low-power system that organizes ECG data. The next stage involves transmitting electrocardiogram signals from a tablet or a phone using the Router over a distant connection or 4G infrastructure. The design of an IoT- based framework is shown in Figure 4.22. The server serves as a conduit in this approach for the expert to get the actual Electrocardiogram data. The system also supports a group of users (specialist/expert workstations) connected to the server via cell phone. ThingSpeak, an open Internet of Things platform, analyses cardiovascular problems using Internet protocols. ThingSpeak is an Internet of Things program that screens information capacity and achieves an ECG signal through a LAN over the web. This technique assists with examining both real-time ECG data

and cloud-based data. ThingSpeak Cloud computing is a sophisticated MATLAB-based program.



Figure 4.21 IoT-based system diagram with sensors, electrocardiogram machine, and smartphone [Reproduced from S. Kumari et.al, 2018]

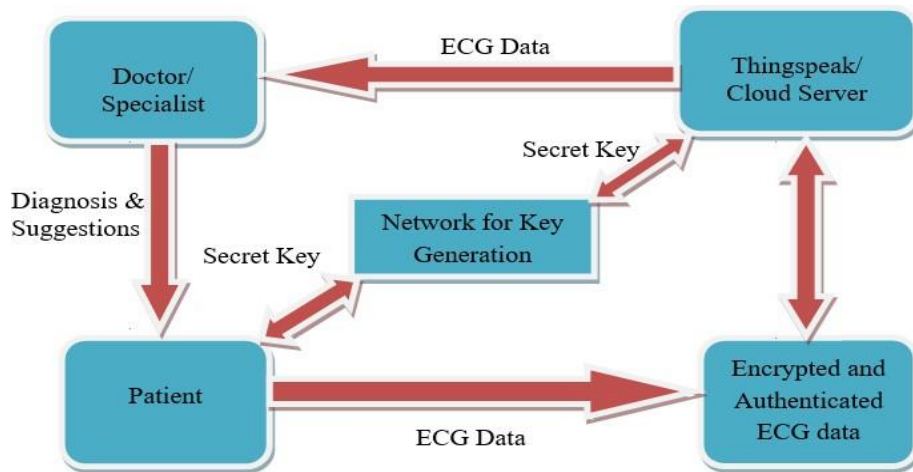


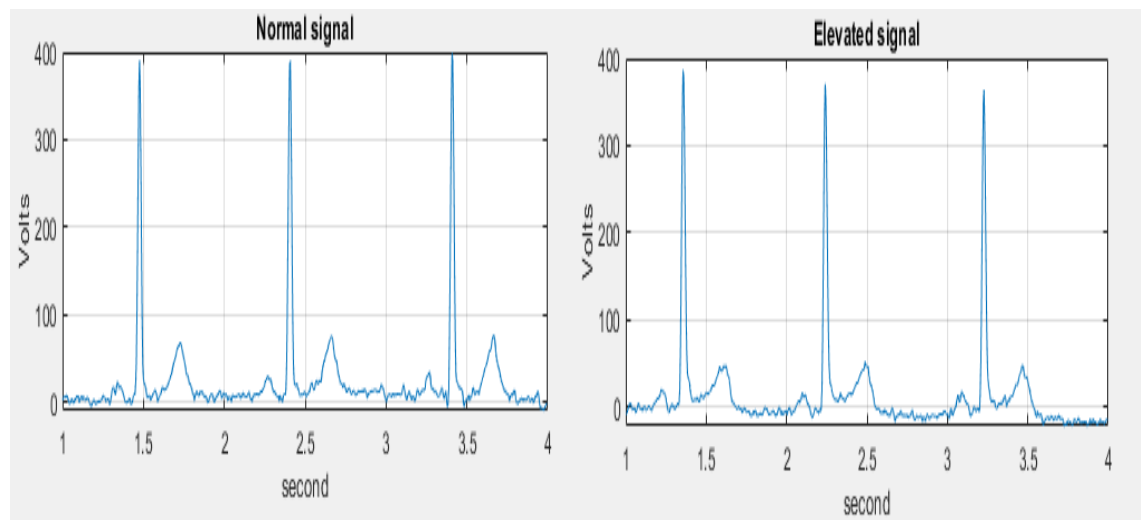
Figure 4.22 Diagram of an IoT-based system [Reproduced from A.K. Sangaiah et.al, 2019]

4.8 Modified Isoelectric Energy Function

The Transition region on an ECG is the region between the onset of ventricular depolarization and its conclusion. In other words, it is the distance between the QRS complex endpoints and the starting of the T wave. The ST segment is the amount of time the cardiac muscle continues to contract to push blood out of the ventricular contraction. One of the most frequent ECG conditions brought on by ischemia is ST divergence (elevation or depression); The height and distress of the ST segment with a standard in the ECG signal are used to evaluate myocardial ischemia close to the implemented lead. Subendocardial infarction is characterized by depressed ST segments (or episodes), whereas transmural (sub-epicardial) ischemia is characterized by increased ST segments [A. Goldberger, 1981]. Figure 4.23 illustrates how the European ST-T database identified the ST- segment (Normal, Elevation) for e0103

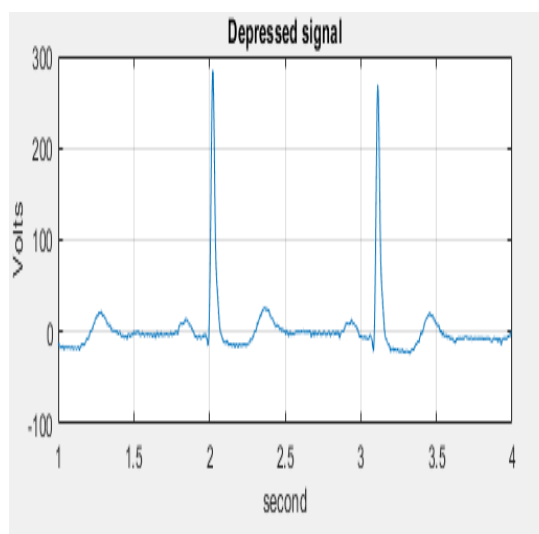
and the depressed signal for e0105.

The work presented here introduces novel strategies for smoothing noised waveforms. The full scheme chart for eliminating low-frequency and high-frequency noise is illustrated in Figure 4.24. In this flow diagram, the data is first loaded from the European ST-T database and normalized the ECG to baseline references and removed the noises using wavelet transforms, followed by the detection of features of the ECG signal and defined the ST segment after that calculation of ST deviation for each beat whether it is normal, elevated, depressed. Then the extracted features are then delivered to clinicians via an IoT cloud channel (Internet of Things) for further analysis.



(a) Normal ST-segment

(b) Ischemic (elevated)



(c) Ischemic (depressed) ST segment

Figure 4.23 (a) Normal ST-segment (b) Ischemic (elevated) ST segment (c) Ischemic (depressed) ST segment

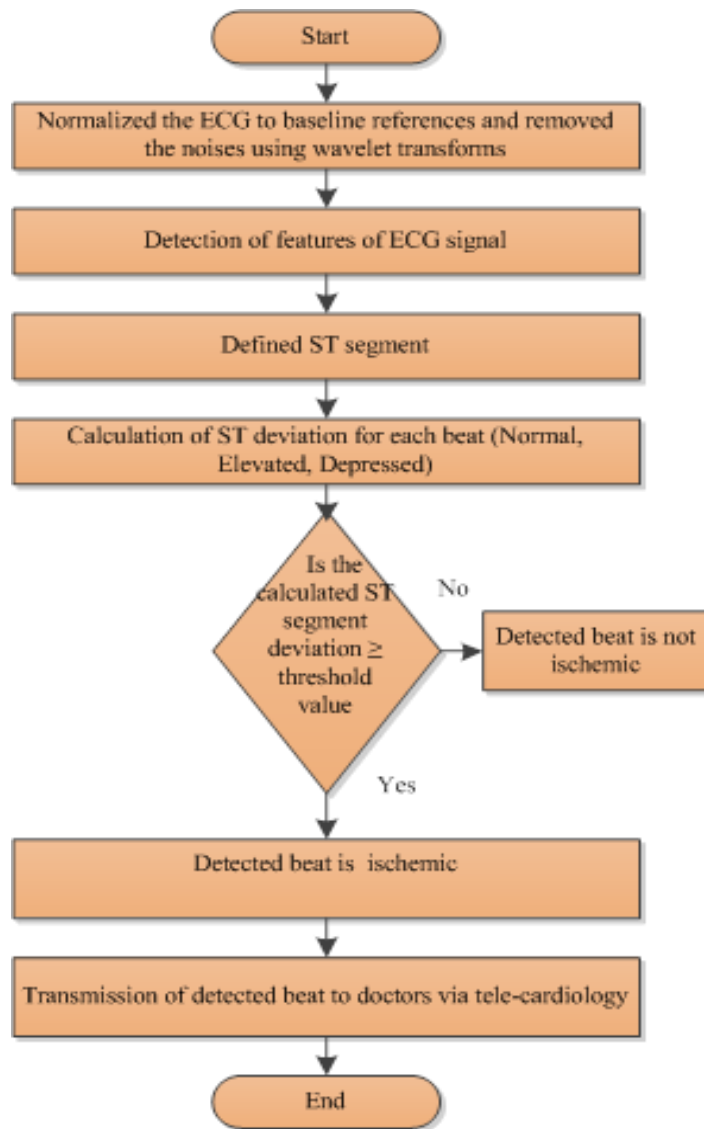


Figure 4.24 Flow chart of the proposed methodology

4.8.1 Deviation in the Region of Interest (ROI) and ST-Segment Assessment

We created a region of interest (ROI) to aid in the appropriate diagnosis of the ST segment and isoelectric reference. The profit of generating ROIs is that only the highest-value samples are used, rather than low-value samples. Depending on the heart rate, the ST segment is defined as the area between the J-point and the Tonset.

Defined ST segment

J+80 ms for heart rate ≤ 120 bpm

J+60 ms for heart rate > 120 bpm

The following is a method for calculating ROI based on the ST segment.

ROI_{ST}

ST segment=length (Jpoint: Tonset)

$M_{ST}=25\%$ of ST Segment

$$ROI_{ST} = J_{point} + M_{ST} : Tonset - M_{ST}$$

The approach is the same for the ROI corresponding to IR.

ROI_{IR}

IR=length (Toffset: Ponset)

$M_{ST}=25\%$ of IR

$$ROI_{IR} = Toffset + M_{ST} : Ponset - M_{IR}$$

The ST Deviation is calculated by potential difference i.e., $ROI_{ST}-ROI_{IR}$ [A. Kumar and M. Singh,2016].

4.8.2 A Novel Modified Isoelectric Energy Measuring Function

A new function for detecting ST deviation has been presented. The modified isoelectric energy function of each sample in the ST segment is evaluated, and a modified isoelectric energy function (MIEEF) is suggested in this study and defined as provided in Eqn. (4.25).

$$MIEEF = \sum \frac{[ROI_{ST} - ROI_{IR} + \alpha]^2}{Length(ROI_{ST})} * \gamma \quad (4.25)$$

where $i=1, 2, 3$ ————up to the number of samples in an ST-segment and 0.01, which is artificially inserted frequently to prevent MIEEF from reaching an infinite value and to keep the categorization threshold of the beat as low as possible. The number of samples in each ST segment of a record is denoted by its length (ST). The MIEEF was created with the idea that samples from segments closest to the baseline will provide more energy than samples from segments further away, and it defined a function to diagnose these differences difficultly instead of detecting the elevation or depression of an ST segment relative to a baseline (isoelectric).

The value of this function should increase as an ST segment approaches the isoelectric reference level and decrease as an ST segment moves below the isoelectric base value. So, a function based on the threshold for detecting myocardial ischemia that we presented in this study [A. Kumar and M. Singh, 2016].

4.8.3 Threshold

In this proposed work, we described the threshold value to differentiate regular beats from myocardial beats in an Electrocardiogram after analyzing iso-electric energy for

each ST segment in the record. An ischemia (elevated or depressed) beat will always have a greater IEEF than a regular beat. Normal heartbeats are denoted by a 1, while ischemic heartbeats are denoted by ± 1 .

If isoelectric energy = 1 then the detected beat is Normal

else if isoelectric energy = -1

then ST segment is depressed

else if isoelectric energy = +1

Then ST segment is elevated

4.8.4 Characterization of Beats

An ischemia beat characterization algorithm has been devised for the records, which filters out fake, following the detection of all potential ischemic or normal beats in the final step. The suggested technique involves the following steps:

- A 120-minute ECG record is segmented into 120 two-minute chunks.
- Each segment is de-noised, defined, and the ST's segments are analyzed.
- Each region should have all of its beats detected and classed as ischemia or normal.
- If a beat is normal, it is given a 1; if it is ischemia, it is given a 0.
- Recombine all sections of the 120-minute ECG record with annotations. The recombination produces an array of L entries, with L denoting the number of beats in a 120-minute ECG record. Each item is either a 0 (ischemic beat) or a 1 (cardiac beat) (for normal beat).
- To create an algorithm for the nth beat where $1 \leq n \leq L$, the record has been expanded with four more entries, two at the start and two at the end. The new record has a -1 at the start and a L+2 at the conclusion. The expanded array will be [-1, 0, 1, 2, ————L, L+1, L+2].
- The extended array is now filtered for erroneous entries using the following procedure from $n=1$ to $n=L$.

The approach is the same for the region of interest (ROI) corresponding to IR.

4.8.5 Detection of Ischemia Episodes

According to the European Society of Cardiology, the ischemia episode diagnosis method should take at least 30 seconds of ECG readings into account. The search for ischemia beats in the whole 60-minute recording begins. A single ischemia episode

must include the following.

4.8.6 Algorithm for Myocardial Infarction (MI) Beat Characterization

Let $S_n = \sum_{k=2} (n + k)$

Where $x(n) = 1$ for a normal nth rhythm and $x(n) = 0$ for a myocardial nth rhythm

If $S_n = \text{three}$, then $x(n) = 1$

Else if $S_n = 0$, then $x(n) = 0$ Else let $P_n = \sum_{k=0} x(n + k)$ If $P_n = 3$, then $x(n) = 1$

Else if $P_n = 0$, then $x(n) = 0$

Else let $T_n = \sum (x(n - 2), x(n - 1), x(n + 1), x(n + 2))$

$T_n = 4$, then $x(n) = 1$

Else if $T_n = 0$, then $x(n) = 0$

Otherwise, the beat is unclassified if $x(n) = 0.5$.

The ischemia window is a segment of a recording that contains at least 90% myocardial rhythms for at least 30 seconds.